Inorganic Chemistry

ARTICLE

pubs.acs.org/IC

Kβ X-ray Emission Spectroscopy Offers Unique Chemical Bonding Insights: Revisiting the Electronic Structure of Ferrocene

Kyle M. Lancaster,*[,†] Kenneth D. Finkelstein,[‡] and Serena DeBeer*[,†]

[†]Department of Chemistry and Chemical Biology, Cornell University, Ithaca, New York 14853, United States

[‡]Cornell High Energy Synchrotron Source, Wilson Laboratory, Cornell University, Ithaca, New York 14853, United States

ABSTRACT: Kβ X-ray emission spectroscopy (XES) is emerging as a powerful tool for the study of chemical bonding. Analyses of the Kβ XES of ferrocene (Fc) and ferrocenium (Fc^+) are presented as further demonstrations of the capabilities of the technique. Assignments of the valence to core (V2C) region of these spectra as electric dipole-allowed cyclopentadienyl (Cp) → Fe 1s transitions demonstrate that XES affords electronic structural insight into the energetics of ligand-based molecular orbitals (MOs). Combined with K-edge X-ray absorption spectroscopy (XAS), we show that XES can provide analogous information to photoemission spectroscopy (PES). Density functional theory (DFT) analyses reveal that the V2C transitions in Fc/Fc^+ derive their intensity from Fe 4p admixture (on the order of 5−10%) into the Cp-based MOs from which they originate. These 4p admixtures confer bonding character to the Cp-based a_{2u} and e_{1u} MOs to at least the extent of backbonding contributions to frontier MOs from higher-lying Cp π* MOs.

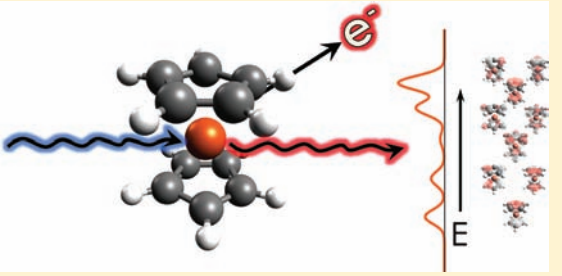

INTRODUCTION

Molecular orbital (MO) theory affords chemists a powerful and intuitive framework for the understanding of chemical bonding and reactivity.[1,2] MO schemes are readily produced by application of group theory[3] to construct bonding, antibonding, and nonbonding combinations of atomic orbitals. In the case of transition metal coordination complexes, these MOs define the extent of metal−ligand interaction. A vast armamentarium of spectroscopic methods are available that permit characterization and energetic localization of these MOs. Generally these techniques focus on the frontier MOs of coordination compounds, e.g., widely used optical spectroscopy is limited to transitions between primarily metal d-orbital-based states and either high-lying ligand bonding and nonbonding MOs or low-lying ligand antibonding MOs. Direct characterization of lower-lying, primarily ligand-based MOs is scarcely encountered; such information typically is extracted from photoemission spectroscopy (PES).[4−6] However, as the technique requires ultrahigh vacuum conditions the sample scope is limited. Herein, we report the utility of Kβ X-ray emission spectroscopy (XES) as a hard X-ray experimental probe of MOs within the primarily ligand-based bonding manifold.

Kβ X-ray emission involves promotion of a 1s electron into the continuum, followed by relaxation of an electron from the 3p manifold to repopulate the resulting 1s core hole via emission of an X-ray photon (Figure 1a).[7,8] Owing to dramatic energy separations of 1s ionization energies, XES is element specific. Kβ X-ray emission spectra may be divided into two regions: the Kβ main line (Fe 7050−7070 eV) with its lower-energy Kβ′ satellite (Fe 7030−7050 eV) and the valence-to-core (V2C) envelope (Fe 7080−7120 eV). Studies from our laboratory comprising a host of Fe complexes have demonstrated that while the Kβ main line and Kβ′ features are primarily influenced by oxidation and spin state, the V2C region additionally exhibits significant sensitivity to coordination environments and ligand electronic structure.[9,10] We will now show that the V2C region affords a direct measurement of the energy separations among states that can be correlated to orbitals of predominantly ligand character within an MO picture. In this manner, V2C XES affords a valuable complement to X-ray absorption spectroscopy (XAS), which directly probes valence states correlated to unfilled orbitals (Figure 1b).

Importantly, Fe XES arises from a metal-centered process. Thus, observation of V2C transitions requires an admixture of metal character into the orbitals comprising the relevant states. Moreover, the intensities reflect the magnitude of these admixtures. The electric dipole moment operator also governs the intensity mechanism. This imposes further selection rules for V2C transitions. Observed V2C features thus arise from states correlated to orbitals containing Fe character that transform with the same symmetry as the electric dipole operator. Application of elementary MO theory permits the prediction and assignment of V2C transitions, which thus afford the energetics of filled ligand-based orbitals as well as metal−ligand covalency. Depending on the molecular point group, this covalency can be decomposed into contributions from not only metal d orbitals but also p orbitals as well. This nicely complements variable-energy PES, which can directly probe metal d character.[11]

Our test cases for this demonstration of the information to be gleaned from V2C XES are the organometallic compounds

Received: April 20, 2011
Published: June 21, 2011

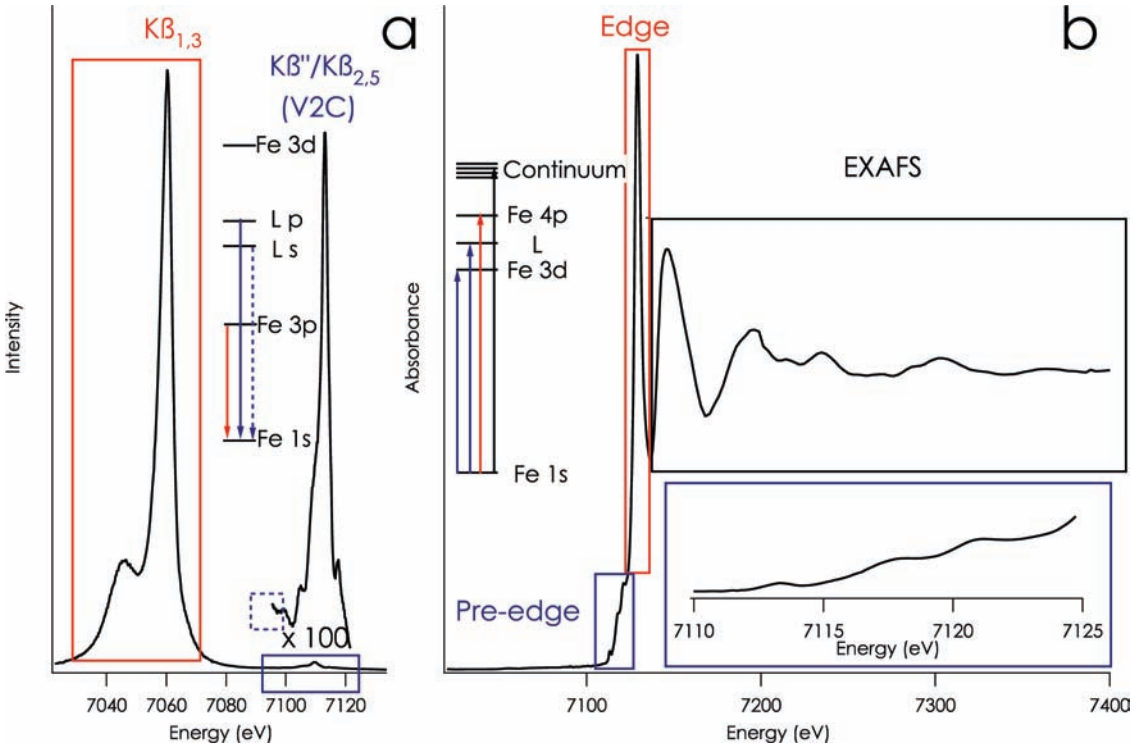

Figure 1. (a) Fe Kβ XES probes electronic transitions to a 1s core hole. Transitions from the Fe 3p orbitals result in the K$\beta_{1,3}$ main line and the Kβ' satellite. These features provide information on Fe spin state. Transitions from primarily ligand np and ns levels give rise to the Kβ'' and K$\beta_{2,5}$ V2C features, respectively. These features are highly sensitive to ligand electronics and molecular symmetry. (b) Fe K-edge XAS probes electronic transitions from the 1s orbital to unfilled orbitals. Pre-edge features arise from weakly allowed 1s to 3d transitions. They can include transitions to unoccupied ligand orbitals. The edge arises predominantly from Fe 1s to 4p transitions. Beyond the edge, extended X-ray absorption fine structure (EXAFS) is observed arising from photoelectron scattering; EXAFS provides information on molecular structure.

ferrocene (Fc) and its one-electron oxidized cation ferrocenium (Fc^+). These molecules are convenient to our purpose as their molecular and electronic structures have been thoroughly characterized.[11−24] This characterization includes PES data, permitting direct comparison with XES results. Not only do our data accord with these previous experiments, but as an extension of previous work, XES and DFT analyses thereof demonstrate the participation of unoccupied Fe 4p orbitals in the chemical bonding of Fc and Fc^+.

MATERIALS AND METHODS

Fc was recrystallized, sublimated, and stored under inert atmosphere. [Fc][BPh_4] (BPh_4 = tetraphenylborate) was synthesized according to a published procedure[25] and dried overnight on a high-vacuum line. It was subsequently brought into a nitrogen-filled glovebox where it was washed with ether and pentane to remove Fc. [Fc][BPh_4] was stored at −35 °C under nitrogen until use. Samples for XES were finely ground in an agate mortar, pressed into 1 mm Al spacers, and sealed with 38 μm Kapton tape. [Fc][PF_6] was used for XAS measurements; it was acquired commercially and used without further purification. XAS samples were diluted in BN to prevent self-absorption, finely ground in an agate mortar, pressed into 1 mm Al spacers, and sealed with 38 μm Kapton tape.

XES Measurements. XES data were obtained at the Cornell High Energy Synchrotron Radiation Source (CHESS) at the C-line end station. The C-line provides an incident flux of ∼2.9 × 10^{12} photons/s at ∼9000 eV in a 1 × 2 mm beam spot. Multilayers were used upstream for energy selection, providing a ∼50 eV band pass at 9000 eV. A Rh-coated mirror was implemented upstream at high angle for harmonic rejection. Kβ X-ray emission spectra were measured using a spherical analyzer (using the 620 reflection of three Ge 310 analyzer crystals) in combination with a silicon drift detector aligned in a Rowland geometry, as described previously.[9] The data were normalized with respect to the incident flux in an N_2-filled ionization chamber just upstream of the samples. The space between the sample, the spherical analyzers, and the detector was filled with helium in order to minimize attenuation of the fluorescence. Data were collected at ∼20 K in a Displex cryostat to minimize photoreduction. In order to assess the rate of photoreduction, short Kβ V2C XES scans were run to determine the acceptable dwell time per sample spot. Only those scans which showed no evidence for photoreduction were included in the final averages. Two scans were employed: "long" scans comprising 360 points with 1 s count times spanned both the Kβ main line (7030.5−7121.7 eV) and the V2C region. "Short" scans comprising 220 points with 3 s count times (7073.3−7121.7 eV) spanned only the V2C region.

The experimental spectra were obtained by first separately averaging long scans and short scans in PyMCA[26] and then merging the resultant average scans together to obtain the full spectra. Energy calibration was performed with a sample of Fe_2O_3. For each of the averaged spectra, the total integrated area was set to a value of 1, and the V2C region was fit using Igor Pro 6.0. Reported V2C areas are multiplied by 1000. The background tail from the Kβ main line and the V2C features were modeled using pseudo-Voigt line shapes. The background from the Kβ main line was subtracted from the reported V2C. Peak areas were determined by integration under each individual curve. The reported areas for individual peaks have an estimated error of 5% based on multiple fits, though the total V2C areas converge to lower uncertainties.

XAS Measurements. Fe K-edge XAS was collected at the Stanford Synchrotron Radiation Lightsource at beamline 7−3 under ring condition

dx.doi.org/10.1021/ic200822b |*Inorg. Chem.* 2011, 50, 6767–6774

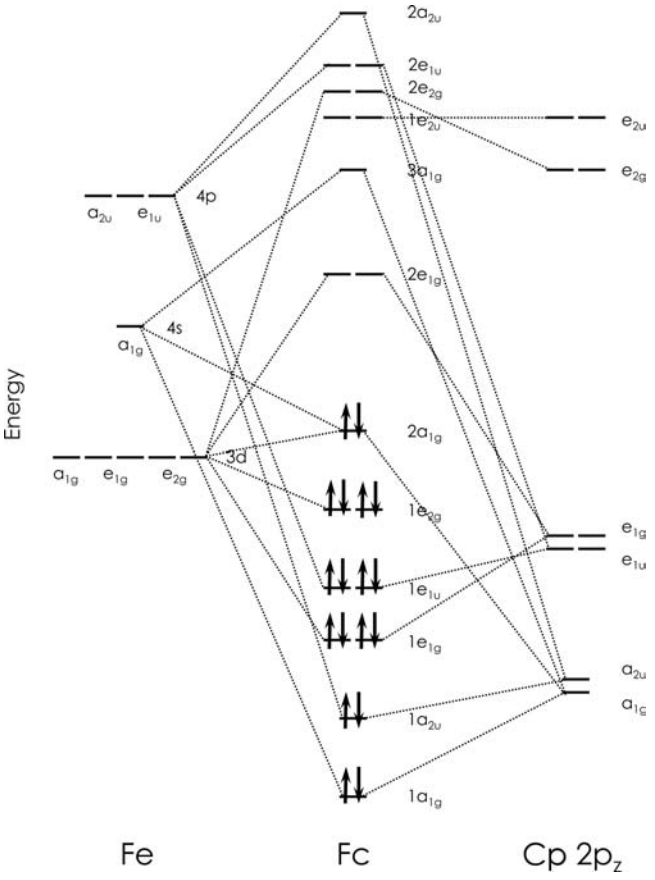

Figure 2. Qualitative Fc MO diagram. Only contributions from the Cp $2p_z$ orbitals are shown; the 2s and $2p_{x,y}$ Cp orbitals transform identically though are shifted to lower energies.

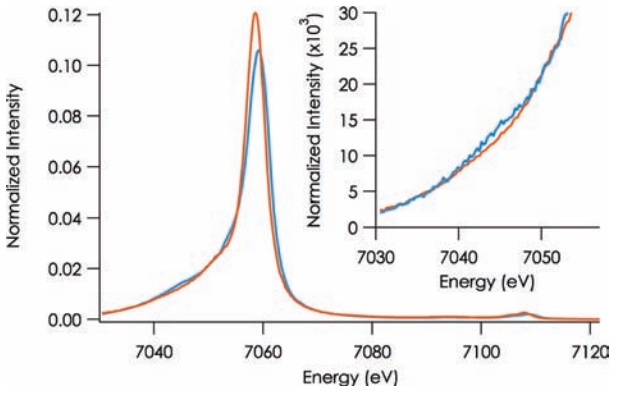

Figure 3. Kβ XES of Fc (orange) and [Fc][BPh_4] (blue). The Kβ' region is inset, showing increased splitting arising from elevated spin state upon oxidation of Fc to Fc^+. Spectra were recorded on undiluted solid samples at 20 K.

of 3 GeV and 300 mA. A Si(220) double-crystal monochromator was used for energy selection, and a Rh-coated mirror (set to an energy cutoff of 9 keV) was used for harmonic rejection. Internal energy calibration was performed by assigning the first inflection point of a Fe foil spectrum to 7111.2 eV. Data were collected in transmission mode using N_2-filled ionization chambers with the sample maintained at 10 K in an Oxford liquid helium flow cryostat. Data were collected from 6785 to 7475 eV ($k = 9.5$ Å^{-1}). Two to four scans were averaged and processed using the

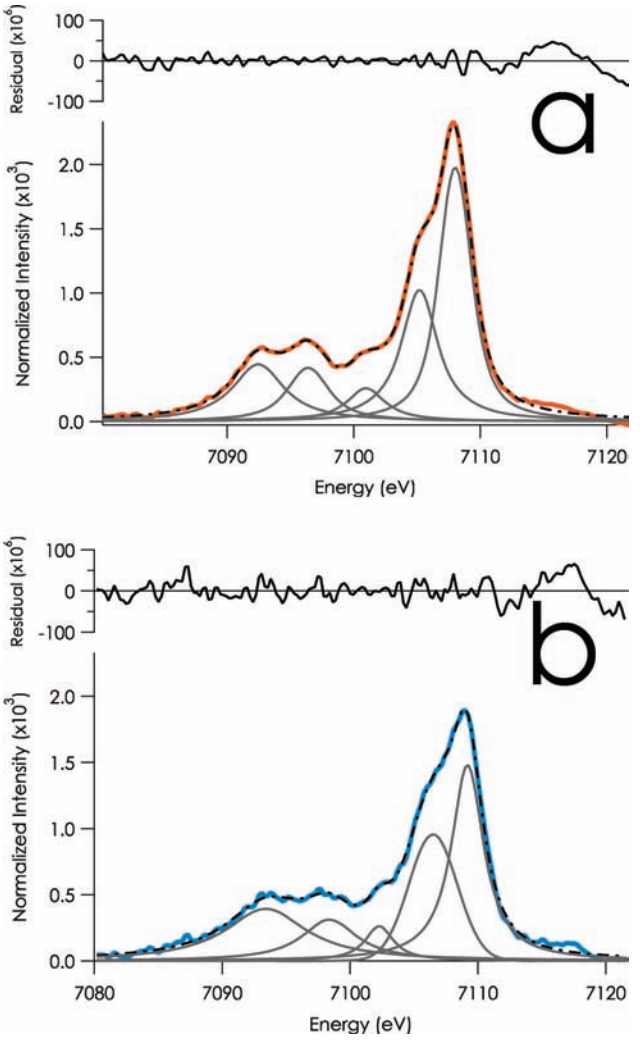

Figure 4. V2C region of (a) Fc and (b) [Fc][BPh_4] Fe Kβ XES. Emission bands were deconvoluted by pseudo-Voigt fitting following subtraction of Kβ main line backgrounds. Fits are overlaid as black dashed lines.

MAVE and PROCESS modules of the EXAFSPAK software package.[27] A smooth pre-edge background was removed from each averaged spectrum by fitting a first-order polynomial to the pre-edge region and subtracting this polynomial from the entire spectrum. All data were normalized to an averaged postedge region of 1. Background from the rising edge was modeled by fitting a pseudo-Voigt line shape at the edge. Pre-edge peak maxima were determined by least-squares fits to the data using Igor Pro 6.0.

Calculations. All electronic structure and spectroscopic calculations were performed using version 2.80 of the ORCA computational chemistry package.[28] Fe V2C XES spectra were calculated on experimental X-ray structures and geometry-optimized structures. Geometry optimizations were performed using the BP86 functional[29,30] with and without empirical van der Waal's corrections, the zeroth-order regular approximation for relativistic effects (ZORA) as implemented by van Wüllen,[31,32] and the scalar-relativistically recontracted def2-TZVP(-f) basis set.[33] Solvation was modeled using the conductor-like screening model (COSMO[34]) using a dielectric of 9.08 (CH_2Cl_2).

XES spectra were calculated using a one-electron theoretical protocol, as described previously.[9] XES calculations were performed using the BP86 functional. The CP(PPP) basis set[31] was used for Fe (with a

dx.doi.org/10.1021/ic200822b |*Inorg. Chem.* 2011, 50, 6767–6774

Table 1. Experimental V2C data for Fc and [Fc][BPh$_4$]

peak	energy (eV)[a]	area[b]
Fc		
1	7092.5	3.2 (15.6)
2	7096.4	2.3 (11.2)
3	7101.0	1.4 (6.8)
4	7105.2	5.4 (26.3)
5	7108.0	8.2 (40.0)
total area		20.5
[Fc][BPh$_4$]		
1	7093.4	4.1 (21.7)
2	7098.4	2.4 (12.7)
3	7102.3	1.1 (5.8)
4	7106.5	4.6 (24.3)
5	7109.2	6.7 (35.4)
total area		18.9
Fc$^+$/Fc intensity ratio		0.92

[a] Instrumental calibration confers a lower limit of 0.2 eV error in band positions. [b] Reported intensities are multiplied by 1000. These values are the result of pseudo-Voigt fits to background-subtracted data. Parenthetical values represent the percentage contribution of each peak to the total intensity. Estimated errors in individual peak areas are on the order of 5%.

special integration accuracy of 7), and the TZVP basis set was used for all other atoms. Solvation was modeled using COSMO in an infinite dielectric. The calculations used a dense integration grid (ORCA Grid4).

RESULTS

Fc/Fc$^+$ MO schemes are typically presented in D_{5d} symmetry representing the staggered conformation. This conformation is in rapid equilibrium with the eclipsed D_{5h} conformation with a barrier to rotation of 0.9 kcal/mol.[14] While removing the inversion center, the change in symmetry to D_{5h} poses negligible energetic consequences to the electronic structure; following convention[19,21,36,37] we will restrict ourselves to a D_{5d} treatment.

The MOs contributing to chemical bonding in Fc/Fc$^+$ arise from linear combinations of cyclopentadienyl (Cp) C 2s and 2p orbitals. In the latter case, MOs comprise mixed linear combinations of atomic orbitals (LCAOs) of C 2p$_x$ and 2p$_y$ orbitals as well as LCAOs of pure C 2p$_z$ parentage. An MO diagram for Fc is presented in Figure 2.[37] In D_{5d} symmetry, the combination of orbitals from the two sandwich-forming Cp ligands transform identically for the entire 2s, 2p$_x$ ± 2p$_y$, and 2p$_z$ set of LCAOs comprising a_{1g}, e_{1g}, e_{2g}, a_{2u}, e_{1u}, and e_{2u} MOs. These may mix with the Fe 3d orbitals transforming as e_{1g}, e_{2g}, and a_{1g} as well as with the Fe 4s (a_{1g}) and Fe 4p (e_{1u}, a_{2u}). Inclusion of the 4p orbitals in MO descriptions of Fc and Fc$^+$ are inconsistent;[39−49] moreover, experimental evidence[16] has suggested that the 4p orbitals do not contribute to the chemical bonding in the compounds.

We now show that Kβ XES can directly address the question of 4p contribution to bonding. The electric dipole operator transforms identically to the p orbitals, that is, as e_{1u} (x,y-polarized) and a_{2u} (z polarized) in D_{5d} symmetry. Conveniently, six ligand-based MOs transform in this manner (vide supra). Recalling that XES intensity is an absorber (i.e., Fe) specific process that is governed largely by the electric dipole operator, it is apparent that observation of transitions involving these MOs

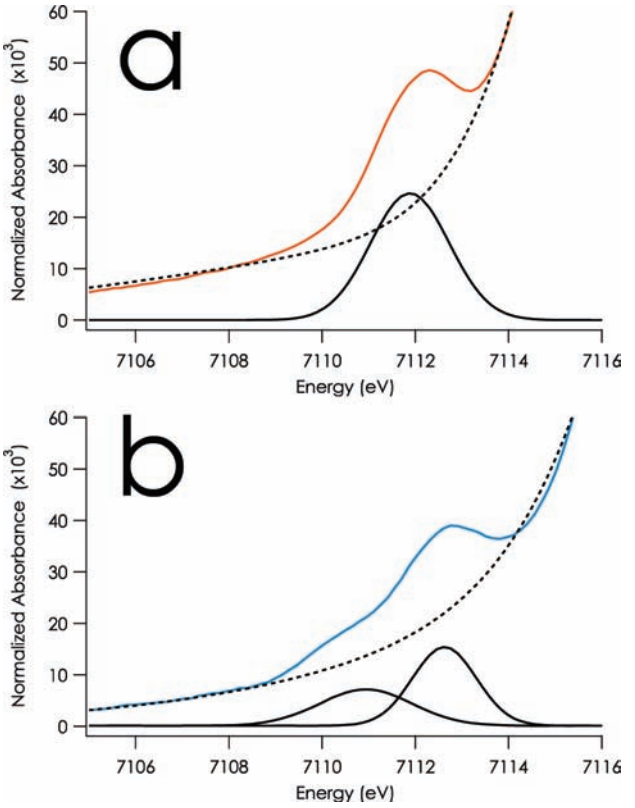

Figure 5. Pre-edge regions of the Fe K-edge X-ray absorption spectra of Fc (a) and [Fc][PF$_6$] (b). Spectra were recorded in transmission mode on solid samples diluted with BN. Dashed lines correspond to backgrounds generated by extrapolating the rising edge line shape as modeled by fitting a pseudo-Voigt peak at the edge.

requires Fe p character in these transitions. Previously we indicated that this p character in V2C transitions arises from the 4p rather than 3p orbitals.[10] Assignment of V2C transitions by calculations and existing data in concert afford confirmation of 4p character in these ligand-based MOs and provide a metric of the magnitude of this admixture.

Kβ X-ray Emission Spectroscopy. The Kβ X-ray emission spectra of Fc and [Fc][BPh$_4$] (BPh$_4$ = tetraphenylborate) are presented in Figure 3. The [Fc][BPh$_4$] Kβ main line at 7059.2 eV is shifted 0.6 eV to higher energy relative to that of Fc at 7058.6. These are consistent with previously reported values for low-spin Fe^{II} and Fe^{III} complexes. The energy shift accords with previous studies of both Fe and Mn coordination compounds that indicate a contribution from increased spin on the order of 0.5−0.6 eV per half unit of spin angular momentum.[9,50] The [Fc][BPh$_4$] Kβ' gains slightly in intensity relative to Fc, a consequence of increased splitting resulting from an increased contribution from 3p−3d exchange brought about by an additional unpaired electron.

The V2C envelopes of both compounds are richly featured, each being fit acceptably to five bands (Figure 4 and Table 1). The [Fc][BPh$_4$] V2C region exhibits 8% lower intensity relative to Fc, as determined by summing the integrated areas of the constituent peaks. This decrease in intensity is consistent with larger metal−ligand separations upon removal of an electron from the e_{2g} π-bonding highest occupied molecular orbital (HOMO) (average R_{Fe-C}: (Fc) = 2.045 Å;[12] (Fc$^+$) = 2.109 Å[13]). The V2C areas for Fc (20.5) and Fc$^+$ (18.9) accord with those determined for low-spin Fe^{II} and Fe^{III} complexes with π-acceptor

dx.doi.org/10.1021/ic200822b |Inorg. Chem. 2011, 50, 6767–6774

ligands, e.g., $Fe^{II}(CN)_6$ = 24.5, $Fe^{III}(CN)_6$ = 21.7.[9] The V2C emission bands are shifted an average 1.3 eV to higher energy upon oxidation of Fc to Fc^+.

K-Edge X-ray Absorption Spectroscopy. K-edge XAS spectra were recorded to facilitate correlation of XES data to existing PES data on Fc/Fc^+ (Figure 5). The preedge region of Fc displays one feature at 7111.9 eV. [Fc][PF_6] shows two preedge features, occurring at 7111 and 7112.6 eV. These absorptions may be assigned as 1s → 3d; the second low-energy feature in the spectrum Fc^+ arises from vacancy in the e_{2g} orbitals upon oxidation. Correspondingly, the higher energy feature corresponds to transitions to the unoccupied e_{1g} orbitals. The 0.7 eV shift of this feature to higher energy in Fc^+ reflects the increased Z_{eff} upon oxidation from Fe^{II} to Fe^{III}.

Density Functional Theory. Kβ X-ray emission spectra were calculated for Fc and Fc^+ using a previously described one-electron model. These calculations were performed on crystallographic and geometry-optimized structures. In the latter case, structures were optimized with and without corrections for van der Waal's dispersion. Structural parameters are presented in Table 2. Although absolute DFT transition energies for core transitions are underestimated due to failure to include relativity and the incorrect modeling of the potential, the relative energy shifts are generally good (within 0.1−0.4 eV).

The calculated XES data for Fc and Fc^+ show remarkable agreement with the experimental spectra (Figure 6, Table 3). The standard deviations of the energy shifts required to align calculated and experimental spectra (0.1 eV < σE < 0.4 eV) approach the limits imposed by instrumental resolution. Moreover, the relative average shifts required to align Fc and Fc^+ spectra calculated using similar protocols (i.e., experimental vs optimized structures) are ≤0.2 eV, indicating that the calculations reproduce the 1.3 eV shift of the V2C to higher energy upon oxidation. Trends in intensity are also reproduced. Notably, the ratios of Fc to Fc^+ V2C intensity are invariant within similar structural categories despite variations among Fe−Ring and Fe−C expansion upon oxidation.

V2C transition assignments are also included in Table 3. The calculations correctly predict that of the six dipole-allowed transitions, only five would be resolved experimentally. The remaining transition is enveloped by the fourth band. Remarkably, even the lowest-lying Cp a_{2u} and e_{1u} MO's contain appreciable (∼10%) Fe p character, affording substantial emission intensities.

Table 2. Structural Parameters for Fc and Fc^+ Used in XES Calculations

method	symmetry	Fe−C (average, Å)	Fe−ring (average, Å)
Fc			
Experiment[12]	D_{5d}	2.045	1.661
BP86-ZORA	D_{5d}	2.058	1.657
BP86-ZORA/VDW	D_{5d}	2.052	1.649
Fc^+			
experiment[13]	D_{5d}	2.109	1.722
BP86-ZORA	D_{5d}	2.109	1.722
BP86-ZORA/VDW	D_{5d}	2.104	1.716

DISCUSSION

The V2C spectra of Fc and [Fc][BPh_4] are richly featured, owing to six dipole-allowed transitions from Cp MO's with as much as 10% Fe p-orbital admixture. While these features were assigned by the application of theory, we may further verify these assignments with characterizations of Fc by PES, XAS, and electronic absorption spectroscopy. Frequently in the discussion of PES data the experimentally observed ionization energies are related directly to orbital energies via Koopmans' theorem.[51] Though we are well aware that experimentally only the many

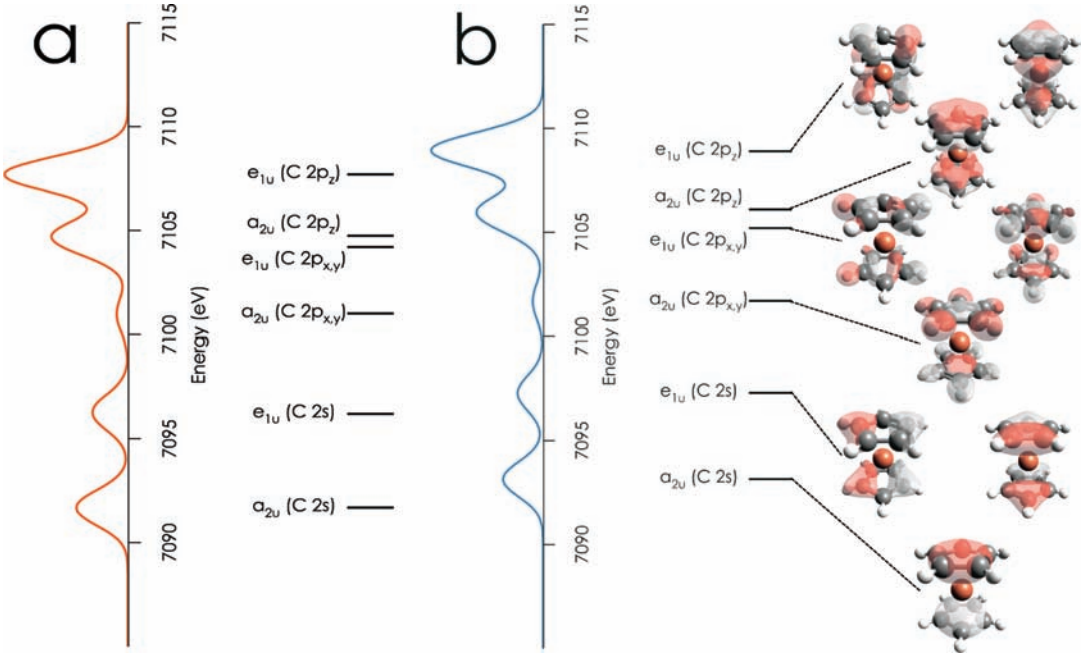

Figure 6. Calculated V2C spectra of Fc (a) and Fc^+ (b) using crystallographically determined molecular structures. MO diagrams are shown featuring the six orbitals from which the majority of the emission intensity originates. The energies of these orbitals are simply the Kohn−Sham one-electron orbital energies derived from the DFT calculations.

dx.doi.org/10.1021/ic200822b |*Inorg. Chem.* 2011, 50, 6767–6774

Table 3. Calculated V2C Data and Assignments for Experimental and Geometry-Optimized Fc and Fc^+ Structures

	experimental[12]		BP86		BP86/VDW			
peak	energy[b] (eV)	intensity[a]	energy[c] (eV)	intensity[a]	energy[d] (eV)	intensity[a]	assignment	%Fe p
Fc								
1	7092.1	37.2 (17.2)	7092.3	36.1 (17.1)	7092.3	37.0 (17.3)	$^2A_{1g} \rightarrow {}^2A_{2u}$ (C 2s)	11.2%
2	7096.6	25.6 (11.8)	7096.6	24.6 (11.7)	7096.5	25.4 (11.9)	$^2A_{1g} \rightarrow {}^2E_{1u}$ (C 2s)	9.6%
3	7101.3	8.0 (3.7)	7101.3	8.6 (4.1)	7101.3	8.7 (4.0)	$^2A_{1g} \rightarrow {}^2A_{2u}$ (C $2p_{x,y}$)	1.7%
4	7105.1	56.6 (26.1)	7105.2	54.1 (25.7)	7105.1	54.6 (25.5)	$^2A_{1g} \rightarrow {}^2E_{1u}$ (C $2p_{x,y}$)	5.1%
							$^2A_{1g} \rightarrow {}^2A_{2u}$ (C $2p_z$)	
5	7108.1	89.2 (41.2)	7107.9	86.9 (41.3)	7107.8	88.6 (41.3)	$^2A_{1g} \rightarrow {}^2E_{1u}$ (C $2p_z$)	18.0%
total area		216.6		210.3		214.3		45.6%
σE	0.3		0.2		0.2			

	experimental[13]		BP86		BP86/VDW			
peak	energy[e] (eV)	intensity[a]	intensity[f] (eV)	intensity[a]	energy[g] (eV)	intensity[a]	assignment	%Fe p
Fc^+								
1	7093.7	30.7 (14.2)	7093.5	30.2 (15.7)	7093.5	31.2 (15.8)	$^3E_{2g} \rightarrow {}^3E_{2u}$ (C 2s)	10.80%
2	7097.8	19.5 (9.0)	7097.9	20.8 (10.8)	7098	21.7 (11.0)	$^3E_{2g} \rightarrow {}^3E_{1u} + {}^3E_{2u}$ (C 2s)	8.60%
3	7102.2	7.9 (3.6)	7102.8	6.5 (3.4)	7102.8	6.5 (3.3)	$^3E_{2g} \rightarrow {}^3E_{2u}$ (C $2p_{x,y}$)	1.40%
4	7106.5	55 (25.4)	7106.3	49.8 (25.9)	7106.4	50.7 (25.7)	$^3E_{2g} \rightarrow {}^3E_{1u} + {}^3E_{2u}$ (C $2p_{x,y}$)	5.50%
							$^3E_{2g} \rightarrow {}^3E_{2u}$ (C $2p_z$)	
5	7109.6	85.9 (39.7)	7109.2	85.1 (44.2)	7109.3	87.1 (44.2)	$^3E_{2g} \rightarrow {}^3E_{1u} + {}^3E_{2u}$ (C $2p_z$)	20.40%
total area	199	199		192.5	185.0	197.1		46.70%
σE	0.1		0.4		0.1			
Fc^+/Fc ratio		0.92		0.91		0.92		

[a] Parenthetical values indicate % contribution to total V2C intensity. [b] Shifted by 182 eV. [c] Shifted by 181.7 eV. [d] Shifted by 181.7 eV. [e] Shifted by 182.2 eV. [f] Shifted by 181.8 eV. [g] Shifted by 181.9 eV.

particle wave functions are observed, the discussion of the results in a one-electron MO-based model greatly simplifies the picture and has also been shown to reasonably model our XES and in this case XAS data as well.[9]

Within this aforementioned approximation, the electrons in the frontier, metal d-orbital based orbitals (following the nomenclature of Figure 1) have binding energies from −3.9 to −4.0 eV ($2e_{1g}$), −6.86 to −6.9 eV ($2a_{1g}$), and −7.21 to −7.23 eV ($1e_{2g}$) as determined in the gas phase by PES.[19,36,37,52] To deeper binding energies are the primarily ligand $1e_{1u}$ orbital at −8.72 to −8.77 eV and $1a_{2u}$ orbital at −12.2 to −12.3 eV. Thus, the separations between the $2e_{1g}$ and the ligand $1e_{1u}$ and $1a_{2u}$ orbitals amount to 4.7−4.9 and 8.2−8.4 eV, respectively. The transition from the Fe 1s to $2e_{1g}$ in Fc was found by XAS to be 7111.9 eV. Combining the information obtained from the XAS (as a reflection of transitions to unoccupied states) and the XES (as a reflection of the occupied states) we obtain $\Delta 2e_{1g} - 1e_{1u}$ and $\Delta 2e_{1g} - 1a_{2u}$ separations of 3.9 and 6.7 eV, respectively. Notably these values are 20% smaller than the values obtained from PES. In a simple picture one may attribute these differences to relaxation, whose effect will be amplified in the presence of a 1s core hole (XAS, XES) as compared to a valence ionization (PES). Similar observations have been made by Solomon and co-workers.[53] Thus, our assignments accord with existing experimental data, indicating that XES may substitute for PES in cases where experimental conditions for the latter technique are untenable.

Previously[10] we demonstrated that the Fe p character that affords dipole-allowed character to V2C transitions originated predominantly from the 4p orbitals. However, we could offer no metric for the contribution of this 4p admixture to chemical bond strengths. Vibronic analysis of the $^2E_{2g} \rightarrow {}^2E_{1u}$ band in the Fc^+ electronic absorption spectrum indicated that the Fe 4p did not participate in chemical bonding, as the Cp−Fe−Cp bond stretching frequency of $^2E_{1u}$ Fc^+ has the same value as $^1A_{1g}$ Fc.[15] This absorption band at 2.01 eV arises from promotion of a $1e_{1u}$ electron to fill the $1e_{2g}$ hole. The difference in energy between the Fe 1s to $1e_{2g}$ XAS feature (7111 eV) and the $1e_{1u}$ to Fe 1s XES feature (7109.2 eV) is in excellent agreement (within error imposed by instrumental resolution) with ΔE = 2.2 eV. Discrepancy between optical and X-ray values is expected to arise from the combination of probing an effectively $3d^{n+1}$ excited state in the case of XAS and energetic relaxation of the 1s level in the case of XES as noted above. Observation of the XES feature necessitates Fe 4p admixture, and by our calculations we estimate ∼20% 4p character in the $1e_{1u}$ orbital. This should stabilize and therefore confer bonding character to this orbital. However, this result is not at odds with the vibronic analysis. The e_{2g} level itself is bonding, stabilized by back-donation from the Cp e_{2g} π^* orbitals. Therefore, no change in stretching frequency should be expected on account of promotion from one bonding level into the next. Thus, the Fe 4p orbitals make a genuine contribution to bonding in Fc of approximately the magnitude of the back-donation from the Cp e_{2g} π^*. A physical consequence of unoccupied p-orbital admixture having been observed, its consequences for structure and reactivity in transition metal chemistry should be investigated further.

dx.doi.org/10.1021/ic200822b |Inorg. Chem. 2011, 50, 6767–6774

CONCLUSIONS

Fe Kβ XES spectra have been recorded for the organometallic compound Fc and its one-electron-oxidized cation [Fc][BPh_4]. The V2C region of the spectra has been assigned using MO theoretical considerations; these assignments are supported by DFT and comparison to earlier PES data. The spectra demonstrate that XES may be used to probe the occupied, Cp-based MOs of these compounds, yielding information analogous to PES but without the requirement of ultrahigh vacuum. Moreover, the spectra provide a qualitative measure of 4p admixture into low-lying Cp-based MOs. V2C XES has been demonstrated as a valuable tool that chemists may exploit to probe filled, ligand-based MOs under fairly unrestrictive experimental conditions. Further such investigations into the bonding of organometallic compounds, including metal carbonyls and alkyl complexes, are underway in our laboratory.

AUTHOR INFORMATION

Corresponding Authors

*E-mail: kml236@cornell.edu; serena.debeer@cornell.edu.

ACKNOWLEDGMENT

We thank Prof. Harry B. Gray for stimulating discussion and Prof. Paul Chirik for providing Fc and [Fc][BPh_4]. We also thank Amb. Stephen Sproules for the Fc/Fc^+ XAS data. The work described herein was funded by an institutional startup grant to S.D. from Cornell University as well by ACS Petroleum Research Fund grant 50270-DN13. This work is based in part upon research conducted at the Cornell High Energy Synchrotron Source (CHESS) which is supported by the National Science Foundation and the National Institutes of Health/National Institute of General Medical Sciences under NSF award DMR-0936384. Portions of this research were carried out at the Stanford Synchrotron Radiation Lightsource (SSRL), a national user facility operated by Stanford University on behalf of the U.S. Department of Energy, Office of Basic Energy Sciences.

REFERENCES

(1) Gray, H. B. *Chemical Bonds: An Introduction to Atomic and Molecular Structure*; University: Sausalito, CA, 1994.
(2) Ballhausen, C. J. *Introduction to Ligand Field Theory*; McGraw-Hill: New York, 1962.
(3) Cotton, F. A. *Chemical Applications of Group Theory*; Wiley: New York, 1990.
(4) Siegbahn, K. *ESCA Applied to Free Molecules*; North-Holland: Amsterdam, 1969.
(5) Siegbahn, K. *Philos. Trans. R. Soc. London A* **1970**, *268*, 33–57.
(6) Turner, D. W.; Baker, A. D.; Baker, C.; Brundle, C. R. *Molecular Photoelectron Spectroscopy*; Wiley: London, 1970.
(7) Glatzel, P.; Bergmann, U. *Coord. Chem. Rev.* **2005**, *249*, 65–95.
(8) de Groot, F. M.F. *Chem. Rev.* **2001**, *101*, 1779–1808.
(9) Lee, N.; Petrenko, T.; Bergmann, U.; Neese, F.; DeBeer, S. *J. Am. Chem. Soc.* **2010**, *132*, 9715–9727.
(10) Pollock, C. J.; DeBeer, S. *J. Am. Chem. Soc.* **2011**, *133*, 5594–5601.
(11) Cooper, G.; Green, J. C.; Payne, M. P. *Mol. Phys.* **1988**, *63*, 1031–1051.
(12) Dunitz, J. D.; Orgel, L. E.; Rich, A. *Acta Crystallogr.* **1956**, *9*, 373–375.
(13) Scholz, S.; Scheibitz, M.; Schödel, F.; Bolte, M.; Wagner, M.; Lerner, H.-W. *Inorg. Chim. Acta* **2007**, *360*, 3323–3329.
(14) Haaland, A.; Nilsson, J. E. *Acta Chem. Scand.* **1968**, *22*, 2653–2670.
(15) Sohn, Y. S.; Hendrickson, D. N.; Gray, H. B. *J. Am. Chem. Soc.* **1971**, *93*, 3603–3612.
(16) Hendrickson, D. N.; Sohn, Y. S.; Duggan, D. M.; Gray, H. B. *J. Chem. Phys.* **1973**, *58*, 4666–4675.
(17) Hendrickson, D. N. *Inorg. Chem.* **1972**, *11*, 1161–1162.
(18) Haaland, A. *Acc. Chem. Res.* **1979**, *12*, 415–422.
(19) Cauletti, C.; Green, J. C.; Kelly, M. R.; Powell, P.; van Tilborg, J.; Robbins, J.; Smart, J. *J. Electron Spectrosc.* **1980**, *19*, 327–353.
(20) Prins, R.; Reinders, F. J. *J. Am. Chem. Soc.* **1969**, *91*, 4929–4931.
(21) Rabalais, J. W.; Werme, L. O.; Bergmark, T.; Karlsson, L.; Hussain, M.; Siegbahn, K. *J. Chem. Phys.* **1972**, *57*, 1185–1192.
(22) Rühl, E.; Hitchcock, A. P. *Inorg. Chem.* **1989**, *111*, 5069–5075.
(23) Wen, A. T.; Rühl, E.; Hitchcock, A. P. *Organometallics* **1992**, *11*, 2559–2569.
(24) Rühl, E.; Heinzel, C.; Baumgärtel, H.; Hitchcock, A. P. *Chem. Phys.* **1993**, *169*, 243–257.
(25) Piglosiewicz, I. M.; Beckhaus, R.; Wittstock, G.; Saak, W.; Haase, D. *Inorg. Chem.* **2007**, *46*, 7610–7620.
(26) Solé, V. A.; Papillon, E.; Cotte, M.; Walter, Ph.; Susini, J. *Spectrochim. Acta B* **2007**, *62*, 63–68.
(27) George, G. N. *EXAFSPAK*; Stanford Synchrotron Radiation Lightsource, Stanford Linear Accelerator Center, Stanford University: Stanford, CA, 2001.
(28) Neese, F., Becker, U., Ganyushin, D., Hansen, A., Liakos, D. G., Kollmar, C., Kossmann, S., Petrenko, T., Reimann, C., Riplinger, C., Sivalingam, K., Valeev, E., Wezisla, B., Wennmohs, F. *ORCA: An ab initio, DFT, and Semiempirical Electronic Structure Package*, version 2.8.0; University of Bonn: Bonn, Germany, 2010.
(29) Becke, A. D. *Phys. Rev. A* **1988**, *38*, 3098–3100.
(30) Perdew, J. P. *Phys. Rev. B* **1986**, *33*, 8822–8824.
(31) van Lenthe, E.; van der Avoird, A.; Wormer, P. E. S. *J. Chem. Phys.* **1998**, *108*, 4783–4796.
(32) van Wüllen, C. *J. Chem. Phys.* **1998**, *109*, 392–399.
(33) Pantazis, D. A.; Chen, X. Y.; Landis, C. R.; Neese, F. *J. Chem. Theory Comput.* **2008**, *4*, 908–919.
(34) Klamt, A.; Schüürmann, G. *J. Chem. Soc., Perkin. Trans.* **1993**, *2*, 799–805.
(35) Neese, F. *Inorg. Chim. Acta* **2002**, *337C*, 181–192.
(36) Evans, S.; Green, M. L. H.; Jewitt, B.; Orchard, A. F.; Pygall, C. F. *J. Chem. Soc., Faraday Trans. II* **1972**, *68*, 1847–1865.
(37) Evans, S.; Green, M. L. H.; Jewitt, B.; King, G. H.; Orchard, A. F. *J. Chem. Soc., Faraday Trans. II* **1974**, *70*, 356–376.
(38) Our MO picture is ordered by the energetics of one-electron orbital energies. Formally, the redox-active molecular orbital for Fc^+ is $1e_{2g}$. The stability of $^2E_{2g}$ relative to $^2A_{1g}$ in Fc^+ arises due to electron pair repulsion. More detailed discussion has been provided: Hendrickson, D. N. *Inorg. Chem.* **1972**, *11*, 1161–1162.
(39) Jaffe, H. H. *J. Chem. Phys.* **1953**, *21*, 156–157.
(40) Dunitz, J. D.; Orgel, L. E. *Nature* **1953**, *171*, 121–122.
(41) Dunitz, J. D.; Orgel, L. E. *J. Chem. Phys.* **1955**, *23*, 954–958.
(42) Moffitt, W. *J. Am. Chem. Soc.* **1954**, *76*, 3386–3392.
(43) Ruch, E. *Recl. Trav. Chim. Pays-Bas* **1956**, *75*, 638–643.
(44) Liehr, A. D.; Ballhausen, C. J. *Acta Chem. Scand.* **1957**, *11*, 207–218.
(45) Shustorovich, E. M.; Dyatkina, M. E. *Dokl. Akad. Nauk SSSR* **1959**, *128*, 1234–1237.
(46) Shustorovich, E. M.; Dyatkina, M. E. *Dokl. Akad. Nauk SSSR* **1960**, *131*, 113–116.
(47) Shustorovich, E. M.; Dyatkina, M. E. *Dokl. Akad. Nauk SSSR* **1960**, *133*, 141–143.
(48) Dahl, J. P.; Ballhausen, C. J. *K. Dan. Vidensk. Selsk. Mat.-Fys. Medd.* **1961**, *33*, 1–22.
(49) Coutière, M.-M.; Demuynck, J.; Veillard, A. *Theor. Chim. Acta* **1972**, *27*, 281–287.

(50) Beckwith, M. A.; Roemelt, M.; Collomb, M.-N.; DuBoc, C.; Weng, T.-C.; Bergmann, U.; Glatzel, P.; Neese, F.; DeBeer, S. Submitted.
(51) Koopmans, T. *Physica* **1934**, *1*, 104–113.
(52) Dowben, P. A.; Waldfried, C.; Komesu, T.; Welipitiya, D.; McAvoy, T.; Vescovo, E. *Chem. Phys. Lett.* **1998**, *283*, 44–50.
(53) Westre, T. E.; Kennepohl, P.; DeWitt, J. G.; Hedman, B.; Hodgson, K. O.; Solomon, E. I. *J. Am. Chem. Soc.* **1997**, *119*, 6297–6314.